

Experimental Limits on Weak Annihilation Contributions to $b \rightarrow ul\nu$ Decays

J. L. Rosner,¹ N. E. Adam,² J. P. Alexander,² K. Berkelman,² D. G. Cassel,² J. E. Duboscq,² K. M. Ecklund,² R. Ehrlich,² L. Fields,² L. Gibbons,² R. Gray,² S. W. Gray,² D. L. Hartill,² B. K. Heltsley,² D. Hertz,² C. D. Jones,² J. Kandaswamy,² D. L. Kreinick,² V. E. Kuznetsov,² H. Mahlke-Krüger,² T. O. Meyer,² P. U. E. Onyisi,² J. R. Patterson,² D. Peterson,² E. A. Phillips,² J. Pivarski,² D. Riley,² A. Ryd,² A. J. Sadoff,² H. Schwarthoff,² X. Shi,² S. Stroiney,² W. M. Sun,² T. Wilksen,² M. Weinberger,² S. B. Athar,³ P. Avery,³ L. Breva-Newell,³ R. Patel,³ V. Potlia,³ H. Stoeck,³ J. Yelton,³ P. Rubin,⁴ C. Cawfield,⁵ B. I. Eisenstein,⁵ I. Karliner,⁵ D. Kim,⁵ N. Lowrey,⁵ P. Naik,⁵ C. Sedlack,⁵ M. Selen,⁵ J. J. Thaler,⁵ E. J. White,⁵ J. Wiss,⁵ M. R. Shepherd,⁶ D. M. Asner,⁷ K. W. Edwards,⁷ D. Besson,⁸ T. K. Pedlar,⁹ D. Cronin-Hennessy,¹⁰ K. Y. Gao,¹⁰ D. T. Gong,¹⁰ J. Hietala,¹⁰ Y. Kubota,¹⁰ T. Klein,¹⁰ B. W. Lang,¹⁰ R. Poling,¹⁰ A. W. Scott,¹⁰ A. Smith,¹⁰ S. Dobbs,¹¹ Z. Metreveli,¹¹ K. K. Seth,¹¹ A. Tomaradze,¹¹ P. Zweber,¹¹ J. Ernst,¹² K. Arms,¹³ H. Severini,¹⁴ S. A. Dytman,¹⁵ W. Love,¹⁵ S. Mehrabyan,¹⁵ J. A. Mueller,¹⁵ V. Savinov,¹⁵ Z. Li,¹⁶ A. Lopez,¹⁶ H. Mendez,¹⁶ J. Ramirez,¹⁶ G. S. Huang,¹⁷ D. H. Miller,¹⁷ V. Pavlunin,¹⁷ B. Sanghi,¹⁷ I. P. J. Shipsey,¹⁷ G. S. Adams,¹⁸ M. Anderson,¹⁸ J. P. Cummings,¹⁸ I. Danko,¹⁸ J. Napolitano,¹⁸ Q. He,¹⁹ H. Muramatsu,¹⁹ C. S. Park,¹⁹ E. H. Thorndike,¹⁹ T. E. Coan,²⁰ Y. S. Gao,²⁰ F. Liu,²⁰ R. Stroynowski,²⁰ M. Artuso,²¹ C. Boulahouache,²¹ S. Blusk,²¹ J. Butt,²¹ J. Li,²¹ N. Menaa,²¹ R. Mountain,²¹ S. Nisar,²¹ K. Randrianarivony,²¹ R. Redjimi,²¹ R. Sia,²¹ T. Skwarnicki,²¹ S. Stone,²¹ J. C. Wang,²¹ K. Zhang,²¹ S. E. Csorna,²² G. Bonvicini,²³ D. Cinabro,²³ M. Dubrovin,²³ A. Lincoln,²³ A. J. Weinstein,²⁴ R. A. Briere,²⁵ G. P. Chen,²⁵ J. Chen,²⁵ T. Ferguson,²⁵ G. Tatishvili,²⁵ H. Vogel,²⁵ and M. E. Watkins²⁵

(CLEO Collaboration)

¹*Enrico Fermi Institute, University of Chicago, Chicago, Illinois 60637, USA*

²*Cornell University, Ithaca, New York 14853, USA*

³*University of Florida, Gainesville, Florida 32611, USA*

⁴*George Mason University, Fairfax, Virginia 22030, USA*

⁵*University of Illinois, Urbana-Champaign, Illinois 61801, USA*

⁶*Indiana University, Bloomington, Indiana 47405, USA*

⁷*Carleton University, Ottawa, Ontario, Canada K1S 5B6 and the Institute of Particle Physics, Canada*

⁸*University of Kansas, Lawrence, Kansas 66045, USA*

⁹*Luther College, Decorah, Iowa 52101, USA*

¹⁰*University of Minnesota, Minneapolis, Minnesota 55455, USA*

¹¹*Northwestern University, Evanston, Illinois 60208, USA*

¹²*State University of New York at Albany, Albany, New York 12222, USA*

¹³*Ohio State University, Columbus, Ohio 43210, USA*

¹⁴*University of Oklahoma, Norman, Oklahoma 73019, USA*

¹⁵*University of Pittsburgh, Pittsburgh, Pennsylvania 15260, USA*

¹⁶*University of Puerto Rico, Mayaguez, Puerto Rico 00681*

¹⁷*Purdue University, West Lafayette, Indiana 47907, USA*

¹⁸*Rensselaer Polytechnic Institute, Troy, New York 12180, USA*

¹⁹*University of Rochester, Rochester, New York 14627, USA*

²⁰*Southern Methodist University, Dallas, Texas 75275, USA*

²¹*Syracuse University, Syracuse, New York 13244, USA*

²²*Vanderbilt University, Nashville, Tennessee 37235, USA*

²³*Wayne State University, Detroit, Michigan 48202, USA*

²⁴*California Institute of Technology, Pasadena, California 91125, USA*

²⁵*Carnegie Mellon University, Pittsburgh, Pennsylvania 15213, USA*

(Received 10 January 2006; published 28 March 2006)

We present the first experimental limits on high- q^2 contributions to charmless semileptonic B decays of the form expected from the weak annihilation (WA) decay mechanism. Such contributions could bias determinations of $|V_{ub}|$ from inclusive measurements of $B \rightarrow X_u l \nu$. Using a wide range of models based on available theoretical input we set a limit of $\Gamma_{WA}/\Gamma_{b \rightarrow u} < 7.4\%$ (90% confidence level) on the WA fraction, and assess the impact on previous inclusive determinations of $|V_{ub}|$.

DOI: [10.1103/PhysRevLett.96.121801](https://doi.org/10.1103/PhysRevLett.96.121801)

PACS numbers: 13.20.He, 12.15.Hh, 12.15.Ji

A precise determination of the magnitude of the Cabibbo-Kobayashi-Maskawa matrix element V_{ub} with well-understood uncertainties is one of the highest priorities in heavy-flavor physics. Recently, significant experimental progress in the determination of $|V_{ub}|$ through inclusive measurements of semileptonic B decays has been achieved with pioneering work such as the incorporation of $b \rightarrow s\gamma$ spectral information for improved modeling [1] and the use of large B -tagged samples [2,3]. Theoretical advances include the quantitative evaluation of the leading and subleading contributions to the partial $B \rightarrow X_u l\nu$ width in restricted regions of phase space [4–14]. Several concerns remain, one of which is the “weak annihilation” (WA) contribution [15–17] to the total $b \rightarrow ul\nu$ rate.

The WA contribution arises from a four-quark operator at order $(\Lambda/m_b)^3$ in the heavy quark operator product expansion in which, crudely, the b quark annihilates within the B meson. Because of an enhancement of $16\pi^2$ relative to other $\mathcal{O}(m_b^{-3})$ operators, WA rate estimates, [15–17]

$$\Gamma_{\text{WA}}/\Gamma_{b \rightarrow u} \approx 0.03 \left(\frac{f_B}{0.2 \text{ GeV}} \right)^2 \left(\frac{B_2 - B_1}{0.1} \right), \quad (1)$$

are a sizeable few percent. A nonzero WA contribution requires violation of factorization for the four-quark operators, parameterized above by $B_2 - B_1$. Little is known about the scale of this violation since it is fundamentally nonperturbative. Because WA is expected to be concentrated in phase space near $q^2 \approx m_b^2$ [15], its *relative* importance is magnified by kinematic requirements that accentuate the high q^2 region to isolate $b \rightarrow u$ from the large $b \rightarrow c$ background. Limiting WA is thus important for understanding the precision of inclusive $|V_{ub}|$ determinations. A probe of the WA scale also tests our overall theoretical mastery of the nonperturbative QCD regime.

In this Letter, we describe a search [18] for a $b \rightarrow ul\nu$ rate at large q^2 , such as would be expected from WA. Our search implicitly averages over contributions from B^\pm and B^0 mesons produced at the $\Upsilon(4S)$. While WA unambiguously predicts a B^\pm and B^0 rate difference, the current precision inclusive $|V_{ub}|$ determinations also average over the charged and neutral mesons, so our results are directly applicable. We use the 15.5 fb^{-1} of data collected at the $\Upsilon(4S)$ resonance with the CLEO II [19], CLEO II.V [20], and CLEO III [21] detectors at the Cornell Electron Storage Ring (CESR). The analysis employs the missing momentum and missing energy techniques used in analyses of semileptonic moments [22,23] and originally developed in studies of exclusive charmless semileptonic decay [24–26]. The procedure takes advantage of the near hermeticity of the CLEO detectors to estimate the four momentum of a single missing neutrino from the missing four momentum $p_{\text{miss}} = (E_{\text{miss}}, \vec{p}_{\text{miss}})$ in an event, where $E_{\text{miss}} \equiv 2E_{\text{beam}} - \sum E_i$ and $\vec{p}_{\text{miss}} \equiv \vec{p}_{\text{CM}} - \sum \vec{p}_i$.

All detector configurations provide acceptance over more than 90% of the full 4π solid angle for both charged

particles (momentum resolution of 0.6% at 2 GeV/ c) and photons (typical π^0 mass resolution of 6 MeV). Charged particles are assigned the most probable mass based on a combination of specific ionization measurements, either time-of-flight or Čerenkov radiation angle measurements, and the relative spectra of π^\pm , K^\pm , and p from B decay. To optimize the missing-momentum resolution, the selection is optimized to identify a single track for each charged particle originating from the B and \bar{B} decays with high efficiency, and to measure energy deposited in the CsI calorimeter that is not associated with charged tracks or their interaction products. The track subset choice is based on event topology rather than individual track quality since high efficiency with minimal double counting is more important than use of only well-measured tracks. Energy clusters located within 8 cm of tracks determined to project into the CsI calorimeter, or consistent with being “split off” from a matched shower, are excluded from the energy and momentum sums.

Electrons satisfying $p > 400 \text{ MeV}/c$ are identified over 90% of 4π using the ratio of cluster energy to track momentum in conjunction with specific ionization (dE/dx) measurements in the main drift chamber. Time-of-flight or Čerenkov measurements provide additional e^\pm/K^\pm separation in the momentum range with ambiguous dE/dx information. Particles in the polar angle range $|\cos\theta| < 0.85$ that register hits in counters beyond 5 interaction lengths are accepted as signal muons. Those with $|\cos\theta| < 0.71$ and hits between 3 and 5 interaction lengths are used in the multiple-lepton veto discussed below. We restrict signal electrons and muons to the range $1.5 < p < 3.0 \text{ GeV}/c$. Within these fiducial and momentum regions the selection efficiency exceeds 90%. The probability of misidentifying a charged hadron as an electron (muon) is about 0.1% (1%).

In events with multiple undetected particles, p_{miss} represents p_ν poorly and causes reconstructed variables in $B \rightarrow X_c l\nu$ decays to smear beyond their kinematic limits into the regions of sensitivity for the much rarer $B \rightarrow X_u l\nu$ process (including WA). This mechanism provides the dominant background contribution in this analysis. Therefore, we reject events with multiple identified leptons, which are usually accompanied by multiple neutrinos. We also reject events with a net charge not equal to zero, or where \vec{p}_{miss} is consistent with particles lost down the beam pipe ($|\cos\theta_{\text{miss}}| > 0.9$).

The missing mass squared $M_{\text{miss}}^2 = E_{\text{miss}}^2 - |\vec{p}_{\text{miss}}|^2$, which should be zero (within resolution) if only a sole neutrino is missing, provides further background suppression. Because the resolution on E_{miss} is about 60% larger than that on $|\vec{p}_{\text{miss}}|$, the M_{miss}^2 resolution $\sigma_{M_{\text{miss}}^2} \approx 2E_{\text{miss}}\sigma_{E_{\text{miss}}}$. Requiring $M_{\text{miss}}^2/2E_{\text{miss}} < 0.2 \text{ GeV}$ provides a zero mass requirement at roughly constant E_{miss} resolution that enhances the signal relative to the background by over a factor of 2. We then take $p_\nu = (E_\nu, \vec{p}_\nu) = (|\vec{p}_{\text{miss}}|, \vec{p}_{\text{miss}})$ in other kinematic calculations. In particu-

lar, we can calculate q^2 , the square of the hadronic momentum transfer in semileptonic decay, via $q^2 = (p_l + p_\nu)^2$. The core resolution on q^2 is about 0.6 GeV^2 , with a broad high-side tail from events with more than one undetected particle.

Finally, we ensure that the event is consistent with $e^+e^- \rightarrow B\bar{B}$ decay. We begin with the standard CLEO hadronic sample, defined by events with at least six primary tracks and a visible energy of at least 20% of the center-of-mass energy. We suppress continuum $e^+e^- \rightarrow q\bar{q}$ backgrounds and $\tau^+\tau^-$ backgrounds using the ratio ($R_2 = H_2/H_0$) of the second to zeroth Fox-Wolfram moments [27] and a sphericity-like variable [28] that is sensitive to momentum flow perpendicular to the lepton, which is small for continuum events. Of the events that satisfy all other criteria and $q^2 > 2 \text{ GeV}^2$, our continuum suppression rejects 72% of continuum while retaining over 90% of semileptonic B decays.

We search for evidence of WA or other sources of high- q^2 $B \rightarrow X_u l \nu$ decays by fitting our measured q^2 spectra in three lepton-momentum bins. The lowest bin ($1.5 < p_l \leq 2.0 \text{ GeV}/c$) is dominated by $B \rightarrow X_c l \nu$ and serves to normalize this background. The total $B \rightarrow X_u l \nu$ yield is determined by the middle ($2.0 < p_l \leq 2.2 \text{ GeV}/c$) and highest ($p_l > 2.2 \text{ GeV}/c$) bins, while the greatest sensitivity for WA-like processes is provided by the highest momentum bin. Our q^2 spectra for the full sample and for the highest momentum bin are shown in Fig. 1. Corrections have been applied for continuum background (using data collected just below $B\bar{B}$ threshold) and for events in which hadrons were misidentified as signal leptons (using data obtained with a lepton veto folded with measured misidentification probabilities).

The corrected q^2 spectra are fitted with $B \rightarrow X_c l \nu$ and $B \rightarrow X_u l \nu$ components obtained from simulation. The $B \rightarrow X_c l \nu$ simulation incorporates all available B -decay data, including measured semileptonic decay form factors. The $B \rightarrow X_u l \nu$ simulation is based on (i) a hybrid model that combines the HQET-based approach of DeFazio and Neubert [24] with known exclusive resonances, and (ii) a simple model for WA that reflects both the kinematics implied by $d\Gamma_{\text{WA}}/dq^2 \sim \delta(q^2 - m_b^2)$ and the intuitive picture where the ‘‘valence’’ quarks in the B meson annihilate and a soft nonperturbative hadronic system X_u materializes. In this formulation, the lepton-neutrino pair carries most of the energy ($q^2 \sim M_b^2$), while the hadronic system has kinematics at the nonperturbative scale Λ_{QCD} . To describe the spectra of that soft hadronic system, our implementation introduces a probability density function (pdf) that is flat out to a cutoff x_0 , where an exponential roll-off with slope Λ begins. The mass M_X and momentum of the hadronic system for a WA decay are drawn independently from this pdf, uniquely determining the kinematics. The system is then hadronized into at least two particles or resonances. Note that since we do not explicitly reconstruct the hadronic final state, the hadronization

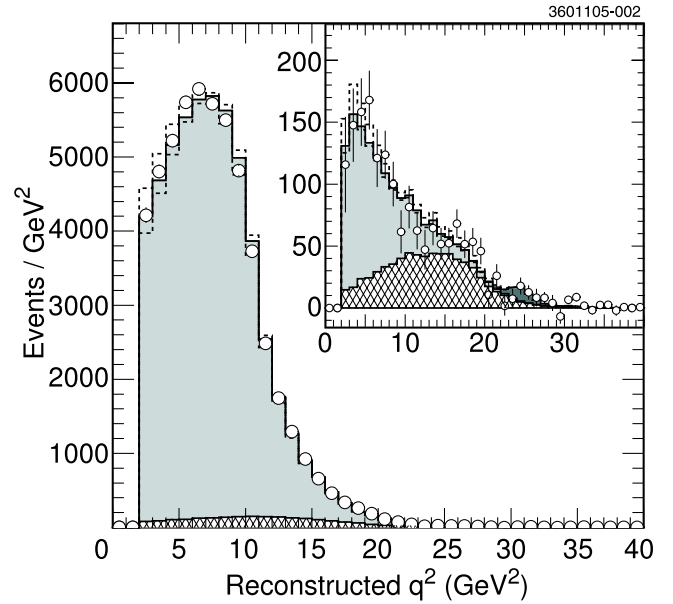


FIG. 1 (color online). The continuum- and fake-lepton-subtracted q^2 spectra (points) for $p_l > 1.5 \text{ GeV}/c$ and $p_l > 2.2 \text{ GeV}/c$ (inset) with components $B \rightarrow X_c l \nu$ (light gray), $B \rightarrow X_u l \nu$ (hatch) and WA (with $\langle M_X \rangle = 0.293 \text{ GeV}$, dark gray). The dashed envelope results from systematic variation of $B \rightarrow X_c l \nu$.

model affects the analysis only through the simulation of the neutrino reconstruction process in the WA Monte Carlo simulation sample, and that through the small variation of detection efficiencies with particle momentum. The kin-

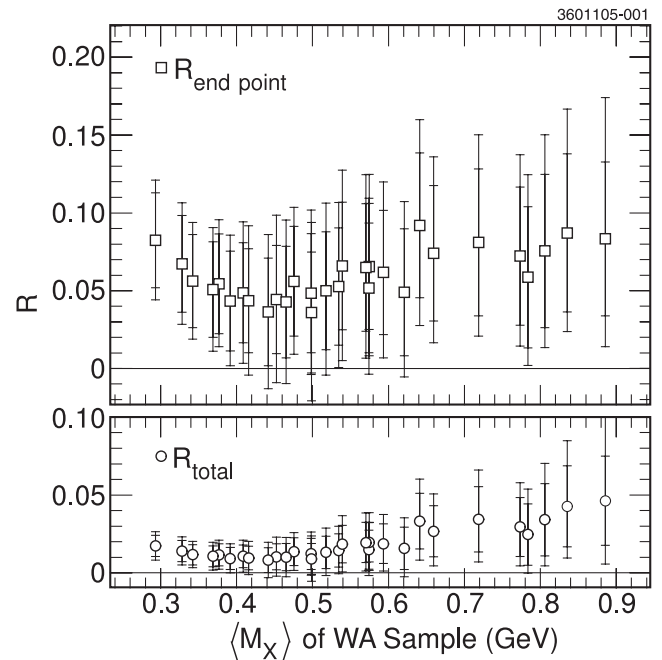


FIG. 2. Fractional size of the WA component for the full phase space (bottom) and restricted to $p_l > 2.2 \text{ GeV}/c$ end point region (top). The statistical (total) uncertainties are represented by the inner (full) error bar.

matics of the $l\nu$ pair are calculated assuming the $V - A$ structure of the weak current and spin $s = 0$ for the hadronic system. We examine combinations of five x_0 and six Λ values, for a total of 30 different WA cases that span a wide range of kinematics.

We perform a separate χ^2 fit for each WA case, with the $b \rightarrow c$, $b \rightarrow u$, and WA rates floating independently. The WA rate is not constrained to be positive. Acceptable fits to the q^2 distributions are obtained for all cases. The $B \rightarrow X_c l\nu$ and non-WA $B \rightarrow X_u l\nu$ components dominate, and in no case is the WA component more than 2 standard deviations above zero (combined statistical and systematic). The most significant WA yield is obtained for the case with $\langle M_X \rangle = 0.293$ GeV (shown in Fig. 1), and appears to result from an overlap with a downward fluctuation in the q^2 distribution of the sample used for continuum subtraction.

From each fit's results for the WA and non-WA $b \rightarrow u$ rates, the ratio $R \equiv \Gamma_{\text{WA}}/\Gamma_{b \rightarrow u}$ is computed for the full phase space (total) and for restricted phase space regions that have been used in previous inclusive $|V_{ub}|$ measurements: $p_l > 2.2$ GeV/ c (end point); $p_l > 1.0$ GeV/ c , $q^2 > 8.0$ GeV² and $M_X < 1.7$ GeV($q^2 M_X$); and $p_l > 1.0$ GeV/ c , $M_X < 1.55$ GeV (M_X). These ratios constrain the extent to which a measured rate can be biased away from current theoretical estimates because of a localized WA contribution. The ratios for the full phase space and end point cases are shown in Fig. 2 and the results for a subset of the cases considered are summarized in Table I. In each region our results, which are statistics

limited, set nontrivial constraints on a localized WA enhancement.

The primary systematic uncertainties arise from experimental effects related to reconstruction of the neutrino, such as the absolute K_L and $b \rightarrow c \rightarrow sl\nu$ rates and spectra, the efficiency and resolution for charged particle and photon detection, modeling and rejection of charged hadronic showers, and charged hadron identification [26]. The $B \rightarrow X_c l\nu$ modeling systematic estimate includes variations of the branching fractions at levels commensurate with recent measurements, and variations of form factors at levels several standard deviations from recent average results [29]. The $B \rightarrow X_u l\nu$ modeling systematic includes a variation of the inclusive shape function similar to Ref. [1] and variation of the X_u hadronization model. In the ratios of the WA component relative to the $B \rightarrow X_u l\nu$ component, many common systematics related to luminosity, fake rates, etc., largely cancel. Table II summarizes the systematic contributions for the WA model shown in Fig. 1. Shifts observed with systematic cross checks such as floating individual components of the $b \rightarrow cl\nu$ background, floating individual classes of mistakes (e.g., extra K_L or extra ν) in the $b \rightarrow cl\nu$ background sample, and even more extreme variations such as eliminating the $Dl\nu$ and non-resonant $b \rightarrow cl\nu$ components are commensurate with the quoted systematics.

To limit the bias in rate measurements quantitatively, we parameterize the variation in the central value and total uncertainty of each WA fraction (R) as a function of $\langle M_X \rangle$.

TABLE I. Summary of “impact ratios” for some WA models considered.

x_0 (GeV)	Λ (GeV)	$\langle M_X \rangle$ (GeV)	R_{total} (%)	$R_{\text{end point}}$ (%)	$R_{q^2 M_X}$ (%)	R_{M_X} (%)
0.30	0.01	0.293	$1.73 \pm 0.68 \pm 0.60$	$8.24 \pm 3.04 \pm 2.34$	$3.89 \pm 1.50 \pm 1.18$	$2.24 \pm 0.88 \pm 0.67$
0.30	0.05	0.328	$1.40 \pm 0.69 \pm 0.58$	$6.73 \pm 3.11 \pm 2.36$	$3.17 \pm 1.52 \pm 1.18$	$1.82 \pm 0.89 \pm 0.66$
0.30	0.20	0.476	$1.36 \pm 0.89 \pm 0.82$	$5.61 \pm 3.52 \pm 3.13$	$3.06 \pm 1.97 \pm 1.77$	$1.76 \pm 1.15 \pm 1.00$
0.30	0.30	0.574	$1.49 \pm 1.25 \pm 1.16$	$5.19 \pm 4.16 \pm 3.82$	$3.33 \pm 2.72 \pm 2.50$	$1.91 \pm 1.58 \pm 1.43$
0.30	0.50	0.773	$2.95 \pm 1.89 \pm 1.89$	$7.23 \pm 4.43 \pm 4.27$	$6.02 \pm 3.74 \pm 3.64$	$3.51 \pm 2.24 \pm 2.13$
0.40	0.01	0.342	$1.17 \pm 0.65 \pm 0.55$	$5.62 \pm 2.98 \pm 2.28$	$2.64 \pm 1.45 \pm 1.13$	$1.52 \pm 0.84 \pm 0.63$
0.40	0.05	0.369	$1.07 \pm 0.67 \pm 0.58$	$5.08 \pm 3.06 \pm 2.51$	$2.42 \pm 1.50 \pm 1.24$	$1.38 \pm 0.87 \pm 0.70$
0.40	0.20	0.498	$1.22 \pm 1.00 \pm 0.96$	$4.85 \pm 3.82 \pm 3.64$	$2.76 \pm 2.22 \pm 2.11$	$1.58 \pm 1.29 \pm 1.21$
0.40	0.30	0.593	$1.88 \pm 1.27 \pm 1.30$	$6.18 \pm 3.99 \pm 4.01$	$4.16 \pm 2.74 \pm 2.76$	$2.39 \pm 1.61 \pm 1.58$
0.50	0.01	0.392	$0.93 \pm 0.71 \pm 0.61$	$4.35 \pm 3.20 \pm 2.70$	$2.10 \pm 1.58 \pm 1.34$	$1.20 \pm 0.91 \pm 0.76$
0.50	0.05	0.416	$0.95 \pm 0.76 \pm 0.75$	$4.36 \pm 3.34 \pm 3.44$	$2.17 \pm 1.69 \pm 1.72$	$1.24 \pm 0.98 \pm 0.99$
0.50	0.10	0.452	$1.03 \pm 0.84 \pm 0.94$	$4.44 \pm 3.48 \pm 4.11$	$2.34 \pm 1.87 \pm 2.16$	$1.34 \pm 1.08 \pm 1.26$
0.50	0.20	0.534	$1.44 \pm 1.07 \pm 1.07$	$5.27 \pm 3.76 \pm 3.73$	$3.25 \pm 2.37 \pm 2.34$	$1.86 \pm 1.38 \pm 1.34$
0.50	0.30	0.621	$1.58 \pm 1.36 \pm 1.32$	$4.90 \pm 4.07 \pm 3.88$	$3.51 \pm 2.96 \pm 2.83$	$2.01 \pm 1.72 \pm 1.62$
0.50	0.50	0.806	$3.42 \pm 2.32 \pm 2.35$	$7.56 \pm 4.91 \pm 4.79$	$6.85 \pm 4.49 \pm 4.42$	$4.04 \pm 2.72 \pm 2.64$
0.60	0.01	0.442	$0.82 \pm 0.80 \pm 0.81$	$3.64 \pm 3.45 \pm 3.55$	$1.87 \pm 1.81 \pm 1.84$	$1.07 \pm 1.04 \pm 1.06$
0.60	0.05	0.465	$1.01 \pm 0.87 \pm 0.91$	$4.28 \pm 3.58 \pm 3.84$	$2.29 \pm 1.96 \pm 2.07$	$1.31 \pm 1.13 \pm 1.19$
0.60	0.30	0.660	$2.67 \pm 1.64 \pm 1.62$	$7.41 \pm 4.34 \pm 4.10$	$5.82 \pm 3.47 \pm 3.32$	$3.38 \pm 2.06 \pm 1.92$
0.60	0.50	0.836	$4.27 \pm 2.61 \pm 2.75$	$8.71 \pm 5.07 \pm 5.10$	$8.44 \pm 4.93 \pm 5.02$	$5.00 \pm 3.03 \pm 3.03$
0.75	0.01	0.518	$1.32 \pm 1.04 \pm 1.10$	$5.01 \pm 3.79 \pm 4.01$	$2.99 \pm 2.31 \pm 2.43$	$1.72 \pm 1.34 \pm 1.40$
0.75	0.20	0.641	$3.33 \pm 1.79 \pm 1.89$	$9.20 \pm 4.65 \pm 4.70$	$7.31 \pm 3.77 \pm 3.85$	$4.27 \pm 2.27 \pm 2.24$
0.75	0.30	0.719	$3.43 \pm 2.09 \pm 2.09$	$8.11 \pm 4.71 \pm 4.45$	$7.38 \pm 4.32 \pm 4.13$	$4.31 \pm 2.61 \pm 2.43$
0.75	0.50	0.886	$4.63 \pm 2.86 \pm 3.80$	$8.34 \pm 4.94 \pm 6.37$	$8.97 \pm 5.28 \pm 6.85$	$5.34 \pm 3.27 \pm 4.20$

TABLE II. Systematic uncertainties (WA model of Fig. 1).

Source	ΔR_{tot}	$\Delta R_{\text{tot}}/R_{\text{tot}}$ (%)
γ efficiency	0.00 177	10.2
Tracking efficiency	0.00 247	14.3
E_γ resolution	0.00 095	5.5
p_{trk} resolution	0.00 134	7.7
K_L multiplicity	0.00 013	0.8
Hadronic shower modeling	0.00 118	6.8
Hadronic shower veto	0.00 065	3.8
Particle identification	0.00 078	4.5
$b \rightarrow c \rightarrow sl\nu$	0.00 020	1.1
$b \rightarrow cl\nu$ modeling	0.00 349	20.1
$b \rightarrow ul\nu$ modeling	0.00 309	17.9
Total	0.00 601	34.7

90% confidence limits (C.L.) are then calculated assuming a flat probability distribution in $\langle M_X \rangle$ over the range we have investigated, resulting in $R_{\text{total}} < 7.4\%$, $R_{\text{endpoint}} < 15.5\%$, $R_{q^2 M_x} < 14.5\%$, and $R_{M_x} < 8.6\%$. Limits on a bias of $|V_{ub}|$ are half these values. These results provide the first concrete constraint on one of the three important uncertainties in extraction of $|V_{ub}|$ for which only indirect bounds [8,30,31] have existed to date. They also place $|V_{ub}|$ from end point analyses on a much stronger footing, where the 8% bound (90% C.L.) we find for a bias in an end-point-based $|V_{ub}|$ is much more restrictive than the conservative bound $\sigma_{\text{WA}} \approx 10\% - 20\%$ [31] and approaches the roughly 5% bound of reference [8]. Studies like these are crucial for inclusive determinations of $|V_{ub}|$ to achieve a 5% precision goal robustly (already achieved statistically).

In summary, we have obtained the first experimental limits on the potential bias in inclusive determinations of $|V_{ub}|$ from a localized contribution to the q^2 distribution, as could arise from weak annihilation. The method presented here is one of several, including study of semileptonic rate differences in the B and $D_{(s)}$ sectors and of the moments of the B semileptonic q^2 distribution [32], that will be needed to understand weak annihilation and its impact upon $|V_{ub}|$.

We gratefully acknowledge the effort of the CESR staff in providing us with excellent luminosity and running conditions. We thank G. Paz, Z. Ligeti, M. Luke, and M. Neubert for helpful discussions. This work was supported by the A.P. Sloan Foundation, the National Science Foundation, and the U.S. Department of Energy.

- [1] A. Bornheim *et al.* (CLEO Collaboration), Phys. Rev. Lett. **88**, 231803 (2002).
 [2] B. Aubert *et al.* (BABAR Collaboration), Phys. Rev. Lett. **92**, 071802 (2004).

- [3] I. Bizjak *et al.* (Belle Collaboration), Phys. Rev. Lett. **95**, 241801 (2005).
 [4] R. D. Dikeman and N. G. Uraltsev, Nucl. Phys. **B509**, 378 (1998).
 [5] I. I. Y. Bigi, R. D. Dikeman, and N. Uraltsev, Eur. Phys. J. C **4**, 453 (1998).
 [6] A. K. Leibovich, I. Low, and I. Z. Rothstein, Phys. Rev. D **61**, 053006 (2000).
 [7] A. K. Leibovich, I. Low, and I. Z. Rothstein, Phys. Lett. B **486**, 86 (2000).
 [8] I. Bigi and N. Uraltsev, Int. J. Mod. Phys. A **17**, 4709 (2002).
 [9] I. I. Bigi and N. Uraltsev, Phys. Lett. B **579**, 340 (2004).
 [10] C. N. Burrell, M. E. Luke, and A. R. Williamson, Phys. Rev. D **69**, 074015 (2004).
 [11] S. W. Bosch, B. O. Lange, M. Neubert, and G. Paz, Nucl. Phys. **B699**, 335 (2004).
 [12] S. W. Bosch, M. Neubert, and G. Paz, J. High Energy Phys., 11 (2004) 073.
 [13] A. H. Hoang, Z. Ligeti, and M. Luke, Phys. Rev. D **71**, 093007 (2005).
 [14] B. O. Lange, M. Neubert, and G. Paz, Phys. Rev. D **72**, 073006 (2005).
 [15] I. I. Y. Bigi and N. G. Uraltsev, Nucl. Phys. **B423**, 33 (1994).
 [16] M. Neubert and C. T. Sachrajda, Nucl. Phys. **B483**, 339 (1997).
 [17] M. B. Voloshin, Phys. Lett. B **515**, 74 (2001).
 [18] T. Meyer, Ph.D. thesis, Cornell University 2005.
 [19] Y. Kubota *et al.* (CLEO Collaboration), Nucl. Instrum. Methods Phys. Res., Sect. A **320**, 66 (1992).
 [20] T. S. Hill (CLEO Collaboration), Nucl. Instrum. Methods Phys. Res., Sect. A **418**, 32 (1998).
 [21] D. Peterson *et al.* (CLEO Collaboration), Nucl. Instrum. Methods Phys. Res., Sect. A **478**, 142 (2002).
 [22] D. Cronin-Hennessy *et al.* (CLEO Collaboration), Phys. Rev. Lett. **87**, 251808 (2001).
 [23] A. H. Mahmood *et al.* (CLEO Collaboration), Phys. Rev. D **67**, 072001 (2003).
 [24] J. P. Alexander *et al.* (CLEO Collaboration), Phys. Rev. Lett. **77**, 5000 (1996).
 [25] M. Athanas *et al.* (CLEO Collaboration), Phys. Rev. Lett. **79**, 2208 (1997).
 [26] S. B. Athar *et al.* (CLEO Collaboration), Phys. Rev. D **68**, 072003 (2003).
 [27] G. C. Fox and S. Wolfram, Phys. Rev. Lett. **41**, 1581 (1978).
 [28] J. D. Bjorken and S. J. Brodsky, Phys. Rev. D **1**, 1416 (1970).
 [29] J. Alexander *et al.* (Heavy Flavor Averaging Group (HFAG)), hep-ph/0412073.
 [30] N. Uraltsev, Int. J. Mod. Phys. A **14**, 4641 (1999).
 [31] S. Eidelman *et al.* (Particle Data Group), Phys. Lett. B **592**, 1 (2004).
 [32] P. Gambino, G. Ossola, and N. Uraltsev, J. High Energy Phys. 09 (2005) 010.